

Electronic Supplementary Materials

ARTICLE

A new route of SERS analysis of intact erythrocytes using polydisperse silver nanoplatelets on biocompatible scaffolds

Received 00th January 20xx,
Accepted 00th January 20xx

Anna A. Semenova,^a Nadezda A. Brazhe,^b Evgeniya Y. Parshina,^b A.S.Sarycheva,^a Georgy V.Maksimov^b and Eugene A. Goodilin^{a,c,d,*}

DOI: 10.1039/x0xx00000x

www.rsc.org/

Superior spectral sensitivity and functional abilities of anisotropic, instead of usually used spherical, noble metal nanoparticles allow to develop new Surface Enhanced Raman Spectroscopy (SERS) approaches to analyse biological objects. We found and resolved for the first time particular risks of survival of silver nanoparticles in different salines to succeed in recording of SERS spectra of intact erythrocytes as an important family of living cells. The ensemble of nanoplatelets with varied shapes and sizes grants multispectral absorption of laser irradiation since a fraction of nanoparticles with a given position of a plasmonic band always exists in such a mixture providing then an effective SERS amplification. At the same time fast recrystallization of anisotropic silver nanoplatelets occurs in a standard chloride - based saline being important to keep the erythrocyte alive but neglecting benefits of the silver platelets as the most versatile and perspective components of SERS sensors. Substitution of chlorides with nitrates keeps both the intact cells and anisotropic nanoparticles safe on biocompatible cellulose SERS scaffolds containing the mixture of silver nanoplatelets thus promoting the development of new SERS devices for biomedical diagnostics.

Experimental details

UV - vis absorption and Raman spectra features of red blood cells. Porphyrin fragments are the vitally important motif of many biological molecules like hemoglobin, myoglobin, cytochromes, catalase, peroxidase enzymes etc.¹⁻⁷, this makes it highly important to prepare and analyze new nanomaterials for successful SERS experiments with biological systems.

In general (Fig.S1, a), heme contains an iron (II / III) ion in the centre of a large porphyrin heterocyclic organic ring composed of four pyrrolic ligands linked cyclically together

by methine bridges. Hemoglobin itself (Hb) possesses a quaternary structure consisting of globin protein subunits in almost a tetrahedral arrangement. Each globin subunit contains porphyrin molecule with the iron ion coordinating nitrogen atoms (N) of the porphyrin in its plane. Besides, the iron ion is also bound to the imidazole N atom of the globin histidine residue below the porphyrin ring. A sixth ligand, an oxygen molecule, binds by one oxygen atom to iron forming oxyhemoglobin (HbO₂). This binding of oxygen pulls the iron into the plane of the porphyrin ring distorting its conformation and then the conformation of the whole Hb molecule. On a cell level, there are at least two populations of Hb molecules inside the erythrocytes with slightly different conformation and functional properties: cytosolic and membrane-bound, or submembrane, hemoglobin (Hb_c and Hb_{sm}, respectively, Fig.S1, b)⁸⁻¹⁰. Hb_{sm} molecules bind to the cytosolic domain of the transmembrane AE1 protein and, therefore, it locates in a close proximity of the surface of erythrocytes (<10-15 nm from the outer surface of the erythrocyte plasma membrane).

^a Faculty of Materials Science, Moscow State University, 119991, Moscow, Russian Federation. Fax: +7 495 939 0998, phone +7 495 939 4609, e-mail:

^b Faculty of Biology, Moscow State University, Moscow, Russia, 119992

^c Kurnakov Institute of General anorganic Chemistry, 119992, Moscow, Russian Federation

^d Faculty of Chemistry, Moscow State University, 119991, Moscow, Russian Federation

† Electronic Supplementary Information (ESI) available: Experimental and characterization details. See DOI: 10.1039/x0xx00000x

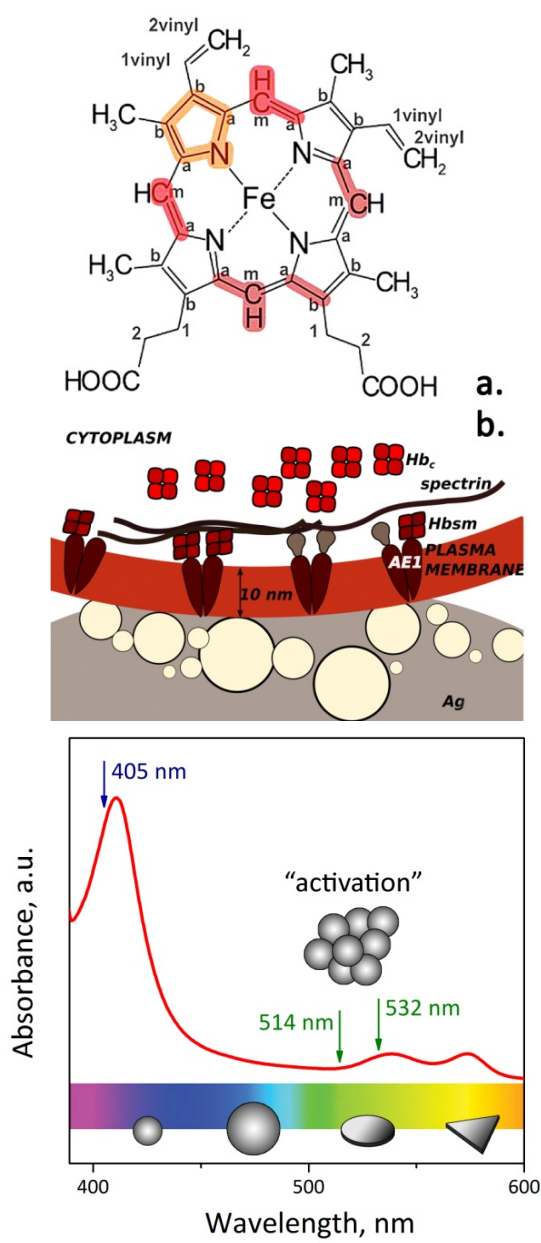


Figure S1. Structural features of red blood cells, (a) a structural formula of heme in hemoglobin, (b) a scheme of the submembrane region of an erythrocyte consisting of a 10 nm thick membrane with adjacent submembrane hemoglobin. Silver nanoparticles (Ag) contact with the outer surface of the membrane. Hbs_m , Hb_c – molecules of the submembrane and cytosolic hemoglobin, respectively; AE1 – an anion exchanger binding Hb and the ankyrin protein that together with the spectrin forms a submembrane cytoskeleton. (c) a scheme comparing experimental absorption bands of oxyhemoglobin (HbO_2), red curve, and plasmonic band regions of silver nanostructures of different morphologies, shapes are given in the bottom of the figure, the arrows show laser excitation wavelengths typically used for SERS experiments, "activation" means nanoparticle aggregation.

The structural peculiarities determine either the absorption or Raman scattering spectra features (Fig.S1-S2). In the oxygenated form, our experimental UV - vis absorbance spectrum of Hb (HbO_2 , Fig.S1, c) corresponds well to the known data and demonstrates three maxima in the visible range: the Soret band, beta- and alpha- bands (about 410, 540 and 575 nm, respectively) originating from the well - established electron transitions in the heme molecule^{4,5}.

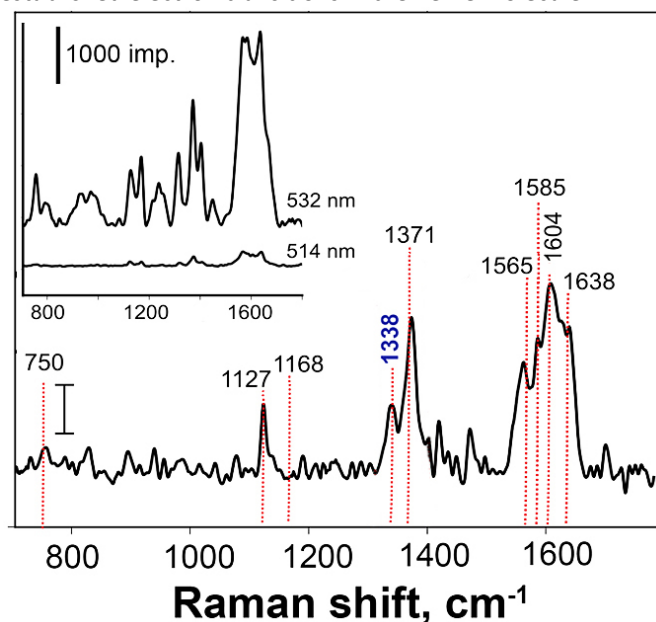


Figure S2. Typical experimental SERS spectra of heme in intact red blood cells in a traditional saline with colloidal nanoparticles (Raman microspectrometer InVia Raman (Renishaw, UK), 532 or 514 nm lasers, excitation power 1.5 mW; objective x5, NA 0.15, registration time 20 s). The inset shows a comparison of same SERS spectra but recorded after shifting the excitation wavelength by about 20 cm^{-1} to achieve resonant conditions.

It is important to note that laser excitation wavelengths for SERS can be used in the regions of Soret and beta-bands (for example, with 404, 417 or 532 nm lasers) leading then to resonant Raman amplification^{6,7,10}. Such conditions favor a much higher enhancement of Raman scattering signal of the analyte if plasmonic nanostructures are also employed in the same regions thus resulting in surface-enhanced resonant Raman spectroscopy^{1-3,10}. The violet laser irradiation fits well either the most bright Soret absorption band or the typical plasmon resonance position of spherical silver nanoparticles (Fig.S1, c). Unfortunately this wavelength damages much biological objects, and is still exotic; also, it is almost impossible to keep single silver nanoparticles separated in chloride salines therefore it is a usual route in many SERS experiments with biological objects to prepare artificially colloidal aggregates with their absorption shifted up to "green lasers" as achieved by their intentional "activation" in sodium chloride solutions^{7,10}. Another successful approach is

based on preparation of hierarchic nanostructured silver materials providing absorption in a wide spectral range¹⁻³. The location of Hb_{sm} on the inner surface of the thin erythrocyte membrane allows a great amplification of the Raman scattering of Hb_{sm} without its direct contact with nanostructures thus giving a possibility to analyse intact cells^{1,3,7,10}. Typical SERS spectra of living red blood cells demonstrate¹⁻³ a set of intensive peaks corresponding to heme molecules at 750, 1127, 1168, 1371, 1565, 1585 and 1638 cm⁻¹. These peaks originate from the normal group vibrations of pyrrol rings, methine bridges and side radicals in the heme^{1-3,7} (Fig.S2, Table S1). It is also important to note that we demonstrated the absence of damage of red blood cells contacting with silver nanoparticles or nanostructured materials, as well as the absence of nanostructure-induced damage of other biological membranes^{1-3,10}.

Table S1. Basic Raman modes of heme as adopted from⁷

Vibration mode, cm ⁻¹	Bonds in heme	Assigned symmetry of vibration	Form of
1635 - 1640	C _a C _m , C _a C _m H, C _a C _b	B _{1g}	HbO2
1620-1623	(C ₁ C ₂)vinyl		HbO2, dHb
1603 - 1608	C _a C _m , C _a C _m H, C _a C _b	B _{1g}	dHb
1580 - 1588	C _a C _m , C _a C _m H	A _{2g}	HbO2
1565 - 1566	C _b C ₁ , C _b C _b	B _{1g}	HbO2
1548 - 1552	C _a C _m , C _a C _m H	A _{2g}	dHb
1502	C _a C _m , C _a C _b , C _a N	A _{1g}	HbO2
1370 - 1375	C _a C _b , C _a N, NC _a N (pyrrol half-ring symmetric)	A _{1g}	HbO2
1345	C ₂ vinylH		HbO2
1172	C _a C _b , C _a N, NC _a N (pyrrol half-ring asymmetric)	B _{2g}	HbO2
1127 - 1045	C _b - CH ₃	B _{1g}	HbO2
754 - 820	heme breathing	B _{1g}	HbO2, dHb

As an example of resonance SERS, we observed a much higher intensity of SERS signal of heme when the laser excitation of 532 nm was used instead of 514 nm (Fig.S2, inset).

Optical features of silver sols with anisotropic particles. Silver sols stabilized with PVP preserve their optical properties for at least 3 - 5 years, the color remains same and no precipitates are observed; main absorption modes are shifted slightly only after 1 - 5 years of storage (Fig.S3).

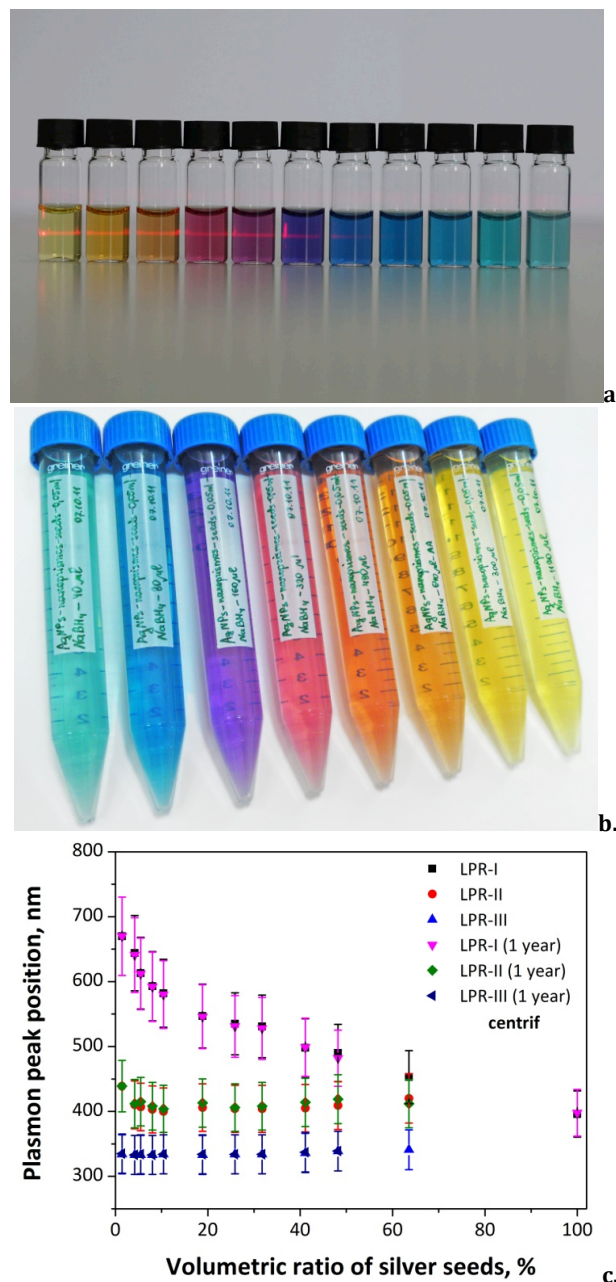


Figure S3. Aged PVP – stabilized silver sols different nanoplatelets stored at 4⁰C in darkness for three (a) or five (b) years, the laser beam disappears in the violet sol being absorbed completely, (c) a negligible shift of main plasmonic bands of silver nanoplatelet sols, used in the main article for preparation of SERS biocompatible substrates, measured for as - prepared samples and after one year of their preparation and storage. The preparation procedure is given in the main article, as adopted from elsewhere¹¹.

The data of Fig.S3 means undoubtedly that silver nanoplatelets do not have a tendency to increase their size or change their shape spontaneously if surfactants and nitrate ions are present in the colloidal solution as the remaining counterpart ions after conducting the silver nanoparticle synthesis. This strong proof of nitrate ion indifference with respect to anisotropic silver nanoparticles is highly contrasting with the behavior of the same sols in the presence of chloride ions as described in the main article.

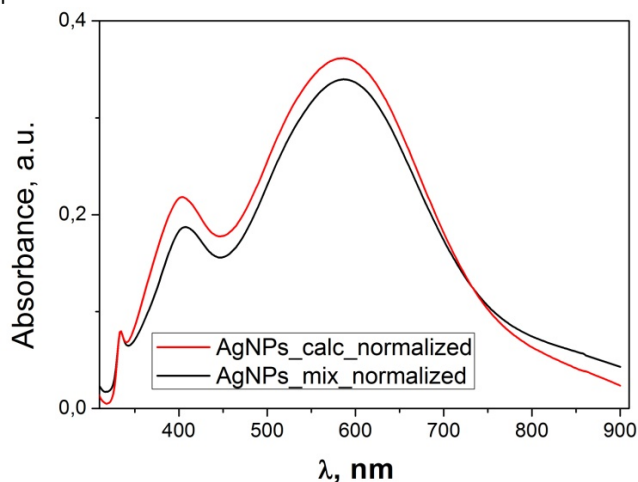
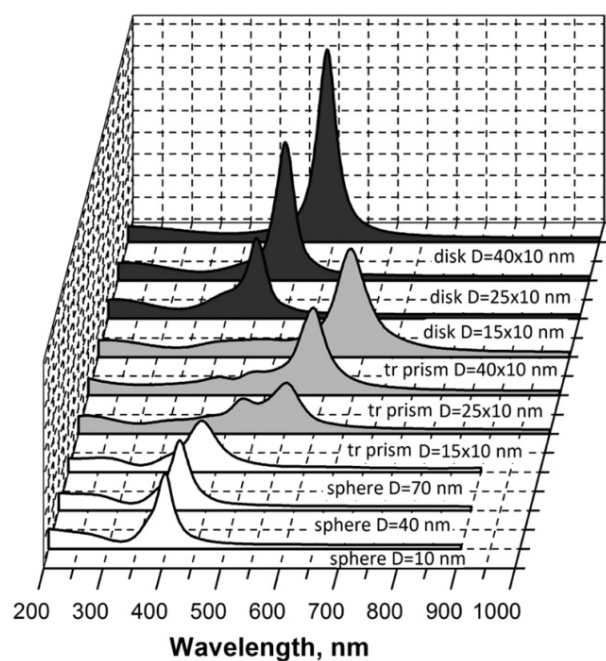
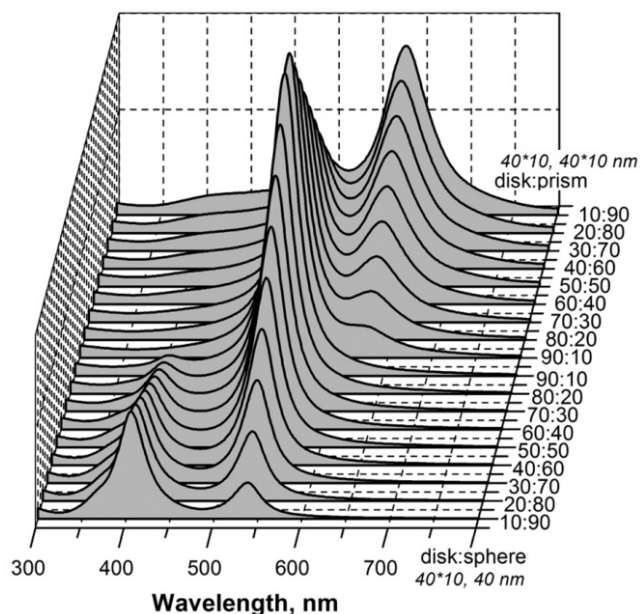


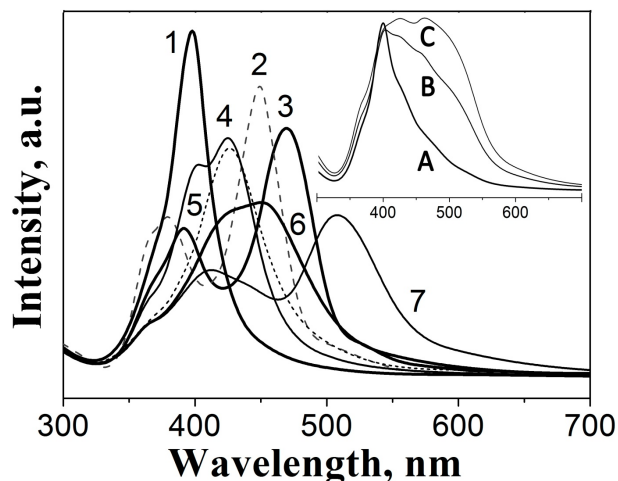
Figure S4. Verification of the additivity features of absorption spectra of nanoplatelet silver sols. The black curve is an experimental absorption spectrum of all the prepared (from yellow to violet) sols mixed together as colloidal solutions in an equal volumetric ratio. The red curve is a normalized mathematical sum of individual spectra of the same sols. The curves are almost identical supporting the fact that there is no interaction or aggregation of the sols when mixing together. Different fractions of silver nanoparticles form a joined ensemble with its own integral optical properties.



a.



b.



c.

Figure S5. DDA simulation of extinction spectra of nanoparticle ensembles with different contributions of anisotropic silver particles; 40*10 nm discs, 40*10 nm triangular prisms and 40 nm spheres are used as components of the overall spectra with given contributions of different fractions of the polydisperse nanoparticle ensemble, (a) single fractions, (b) mixtures of the fractions. The contributions are given in the picture, (c) plasmonic bands for a mixture of 70*70*105, 40*40*60, 70*70*84, 40*40*48 nm ellipsoids and 10 nm spheres with contributions (%) of 10:10:10:30:50 (A), 35:10:35:10:10 (B) and 50:20:20:10:0 (C), respectively in the inset; spectral components of the simulated spectra, 10 nm (1) and 70 nm (5) spheres, 10*10*15 nm (2), 40*40*60 nm (3), 40*40*48 nm (4), 70*70*84 (6), 70*70*105 nm (7) ellipsoids, respectively.

In addition to the outstanding colloidal and chemical stability of the original sols (Fig.S3), we have to note their additivity feature which exists obviously: Fig.S4 demonstrates that all the measured absorption spectra are only an integral

property of large nanoparticle ensembles while SERS amplification is caused mostly by a proper fraction of nanoparticles (Fig.S1, c, Fig.S2). To clarify the statement of additivity as a property of the absorption spectra of silver nanoplatelet ensembles, the discrete dipole approximation (DDA) method was used to simulate optical properties of the silver sols as based on the DDSCAT 7.1 software¹² for aqueous surrounding and the number of dipoles equal to $6 \cdot 10^4 - 9 \cdot 10^4$ (Fig.S5). It is assumed that each nanoparticle makes its own contribution to the extinction spectrum independently on the neighbor particles in diluted sols, as seen experimentally (Fig.S4). This assumption gives the possibility to compute the extinction spectrum of the particle ensemble additively, as a sum of the individual particle contributions. The DDA method is known to be a quite useful and versatile computational tool for particles with arbitrary shapes. As evident from Fig.S5, an ensemble of spherical particles can not physically give a broad extinction spectrum observed experimentally since isotropic particles give a very narrow plasmon peak and, moreover, this narrow peak shifts only by 15 - 20 nm to the red side even if the particle size becomes several times larger, as also shown schematically in Fig.S1, c. If large slightly anisotropic silver nanoparticles are present, while a fraction of the smallest isotropic 10 nm nanoparticles is negligible (Fig.S5), the spectrum is broadened, more absorption and scattering occur at the blue and red ends of the spectrum. Actually there is always a possibility that any median of the spectra corresponds to nothing real in terms of an exact size and shape of the nanoparticles since this is (might be) a sum curve of different contributions from several fractions of the nanoparticle ensemble.

On the other hand, it is known that SERS amplification for intact biological objects demands definitely a physical contact of the object and the nanostructures since the SERS effect vanishes quickly on the distances more than 15 - 20 nm¹⁻³. As mentioned above (Fig.S1, S2), the resonant effects play a great role in the analysis of erythrocytes or, in general, most of biological objects and analytes. Therefore it does not really matter how broad the nanoparticle distribution is, since only a proper fraction of nanoparticles matching both the absorption range of the analyte molecule and the laser excitation wavelength will work. As a simple hypothetical example, if the resonant effect is observed even for one percent of such "proper nanoparticles" contacting with erythrocytes, it then leads to $10^3 - 10^4$ fold better amplification of the Raman signal because of the resonance, therefore the rest 99% of the nanoparticles will contribute roughly 10% (or less) of the overall SERS amplification only. This assumption leads to the main idea of the current article on creation of an universal biocompatible substrate for SERS analysis of biological objects and erythrocytes, in particular, which can be achieved under several conditions only:

(1) a mixture of anisotropic silver nanoparticles is used to achieve a broad integral absorption (like in Fig.S4 or in the main article for the finally prepared cellulose substrate) with

more or less uniform contributions of many fractions of nanoparticles being suitable for a given analyte and also widespread excitation lasers,

(2) nanoparticles are immobilized on a biocompatible scaffold to increase a contact area with living cells and to reduce the ability of nanoparticles to mutually aggregate as it leads usually to unpredictable changes of their optical properties in a solution,

(3) nanoparticle surrounding does not affect their size and, more importantly, their shape thus keeping all the benefits of nanoplatelets in terms of advanced plasmonic modes and SERS effectiveness.

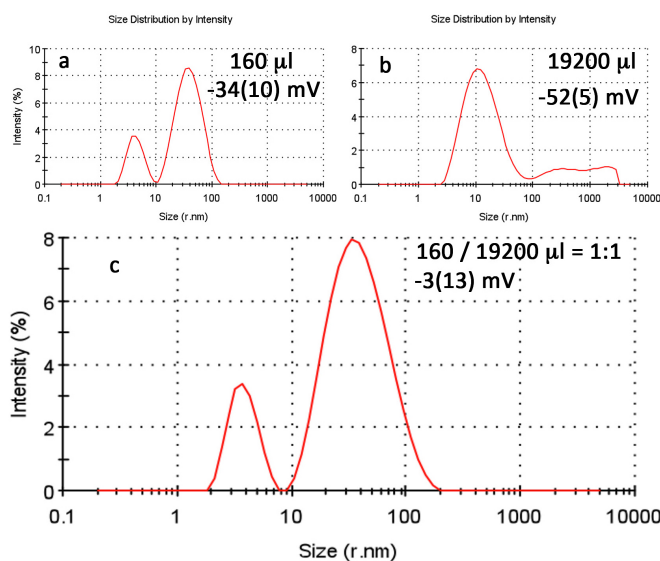


Figure S6. Typical DLS data and zeta - potential estimation for silver nanoplatelet sols. (a) a 160 microliter aliquot of seeds, a violet - aquamarine sol with large silver nanoplatelets, (b) a 19200 microliter aliquot of seeds, a yellow - orange sol, (c) a mixture of (a) and (b) in a ratio of 1:1.

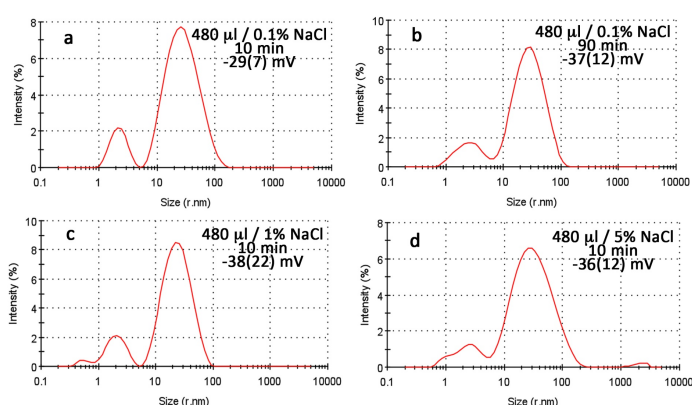


Figure S7. Typical DLS data and zeta - potential estimation for silver nanoplatelet sols prepared using a 480 microliter aliquot of seeds, violet - blue sol with large anisotropic silver platelets treated with different concentrations of sodium chloride solution added.

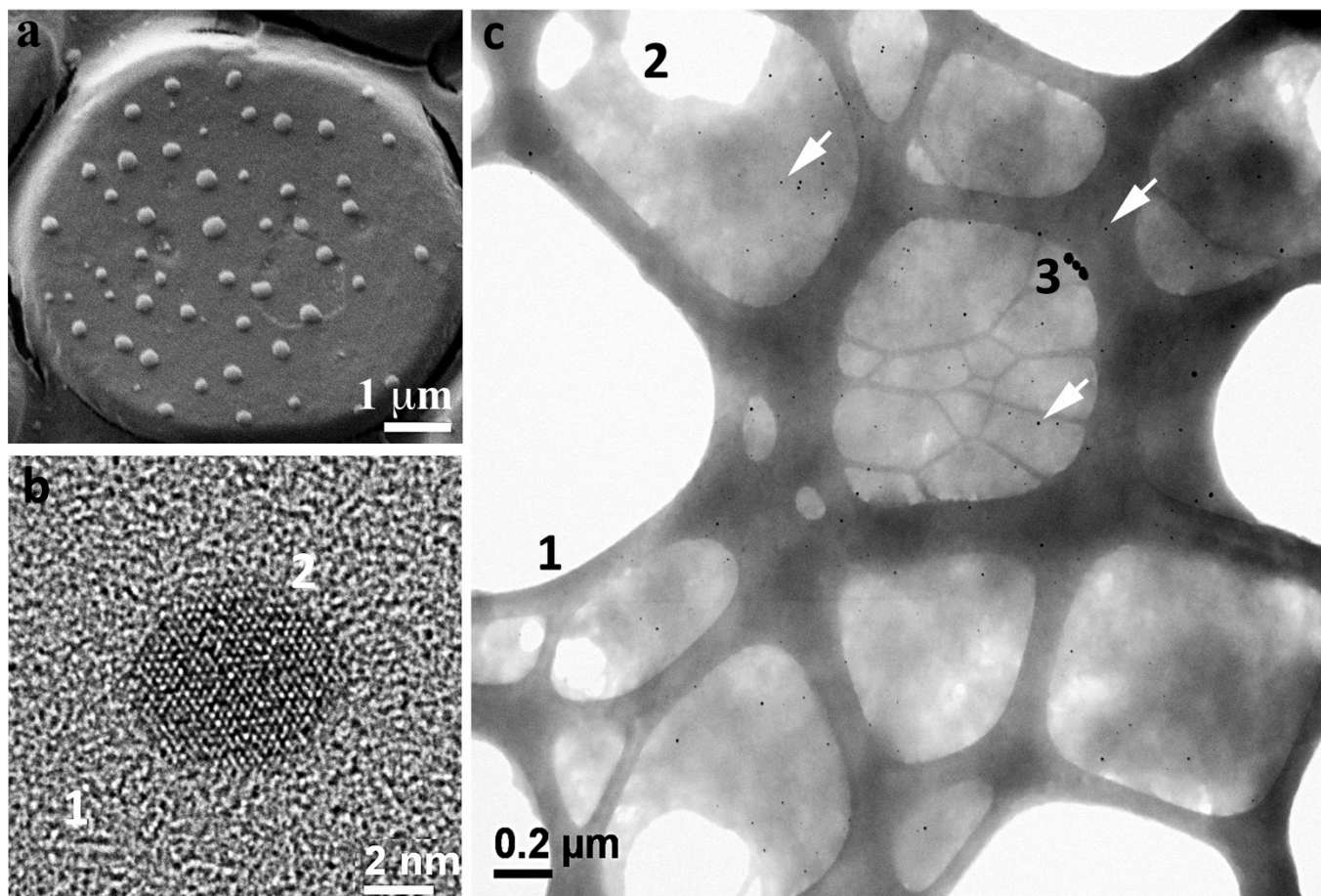


Fig.S8. Interaction of silver nanoparticles with erythrocyte membranes. (a) a general view of erythrocytes mixed with silver hydrosol, exposed for 10 min., centrifuged and stabilized with 5% glutaraldehyde for SEM imaging, (b) a TEM image of a part of erythrocyte membrane (1) with a small silver nanoparticle (2), (c) a general view of erythrocyte ghosts (vesicles of erythrocyte membranes free from Hbc) mixed with silver hydrosol, exposed for 10 min., centrifuged and stabilized with glutaraldehyde for TEM imaging, "1" marks an edge of TEM mesh, "2" corresponds to the edge of erythrocyte membrane (host), "3" - large silver nanoparticles onto the membrane, smaller AgNPs are marked with arrows.

Fig.S6 and Fig.S7 demonstrate some features of the silver sols as seen from a point of view of dynamic light scattering (DLS). Unfortunately, such data are not precise and distinct since DLS software uses usually an approximation of all measured objects by spheres. Therefore such DLS data becomes less sensitive to the observed changes in the nanoparticle sizes and shapes as compared to alternative analytical methods described above and in the main article.

Silver sol mixtures with red blood cells. The most important criterion of erythrocyte stability in the presence of silver nanoparticles is overall and shape integrity of red blood cells. Any membrane defect has a chance to result in hemoglobin leakage followed by erythrocyte shrinkage and shape distortion. Therefore, microscopic observation of all the cells and their step - by - step counting seems to be an important way of answering a question about silver "toxicity" for these highly important biological objects. We have already

presented several techniques of erythrocyte analysis in this contest^{1-3,10} while new results are given in the main article.

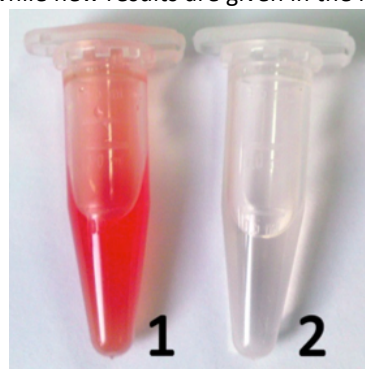


Fig.S9. One hundred fold diluted (1) and finally 3000 fold diluted blood (2) used for the SERS analysis.

In addition, Fig.S8 represents how silver nanoparticles interact with the outer surface of erythrocyte membranes. If the nanoparticles are free and surrounded by electrolytes,

they aggregate and can stuck to the surface of cells. Some recent works¹³ consider that the cytotoxicity of aggregated nanoparticles is significantly higher than well-dispersed ones. The dispersity-dependent cytotoxicity may be related to the increase of cellular endocytosis and formation of reactive oxygen species. At the same time (Fig.S8), our results demonstrate that even small silver nanoparticles themselves are not damaging objects for the erythrocytes, at least in terms of mechanical destruction of the membranes and pronounced chemical interactions with lipids. Preparation of silver nanoplatelets of a larger size to reach the beta - band of HbO₂ and also their deposition on a biocompatible scaffold, as described in the main article, would give a further surplus in the silver nanoplatelets biocompatibility. Fig.S9 gives a visual impression about the dilution level of red blood samples used for SERS analysis in the main paper. The right side sample in the nitrate / chloride - based saline is white - rose, almost colorless, although it will become immediately reddish if something damages the cells.

References

1. A. A. Semenova, E. A. Goodilin, N. A. Brazhe, V. K. Ivanov, A. E. Baranchikov, V. A. Lebedev, A. E. Goldt, O. V. Sosnovtseva, S. V. Savilov, A. V. Egorov, A. R. Brazhe, E. Yu. Parshina, O. G. Luneva, G. V. Maksimov, Yu. D. Tretyakov, *J. Mater. Chem.*, 2012, **22** (47), 24530.
2. N.A. Brazhe, A.B. Evlyukhin, E.A. Goodilin, A.A. Semenova, S.M. Novikov, S.I. Bozhevolnyi, B.N. Chichkov, Asya S. Sarycheva, A.A. Baizhumanov, E.I. Nikelshparg, L.I. Deev, E.G. Maksimov, G.V. Maksimov, O. Sosnovtseva, *Scientific Reports*, 2015, **5**:13793, DOI: 10.1038/srep13793
3. A. S. Sarycheva, N. A. Brazhe, A. A. Baizhumanov, E. I. Nikelshparg, A. A. Semenova, A. V. Garshev, A. E. Baranchikov, V. K. Ivanov, G. V. Maksimov, O. Sosnovtseva, E. A. Goodilin, *J. Mater. Chem. B*, 2016, **4**, 539.
4. B.L. Horescer, *J.Biol.Chem.*, 1943, **148**, 183.
5. W.G. Zijlstra, A. Buursma, Spectrophotometry of hemoglobin: Absorption spectra of bovine oxyhemoglobin, deoxyhemoglobin, carboxyhemoglobin, and methemoglobin. In: *Comparative biochemistry and physiology B - Biochemistry & molecular biology*, 1997, **118** (4), 743.
6. B.R. Wood, B. Tait, D. McNaughton. *Biochimica et Biophysica Acta*, 2001, **1539**, 58.
7. N. A. Brazhe, E. Y. Parshina, V. V. Khabatova, A. A. Semenova, A. R. Brazhe, A. I. Yusipovich, A. S. Sarycheva, A. A. Churin, E. A. Goodilin, G. V. Maksimov, O. V. Sosnovtseva, *J. Raman. Spectr.*, 2013, **44** (5), 686.
8. N. Shaklai, J. Yguerabide, H.M. Ranney, *Biochemistry*, 1977, **16**, 5585.
9. Q. Chen, T. C. Balazs, R. L. Nagel, R. E. Hirsch, *FEBS Lett.*, 2006, **580**, 4485.
10. N.A.Brazhe, S. Abdali, A.R.Brazhe, O.G. Luneva, N.Y. Bryzgalova, E.Y. Parshina, O.V. Sosnovtseva, G.V. Maksimov, *Biophys J.*, 2009, **97** (12), 3206.
11. J. Zeng, J. Tao, W. Li, J. Grant, P. Wang, Y. Zhu, Y. Xia, *Chemistry - An Asian Journal.*, 2011, **6**(2), 376.
12. B.T. Draine, P.J. Flatau, *J. Opt. Soc. Am. A*, 1994, **11**, 1491.
13. D. Huang, H. Zhou, H. Liu, J. Gao, *Dalton Trans.*, 2015, **44**, 17911.